CORRELATIONS BETWEEN THE RELATIVE CORROSION INHIBITION EFFECT AND THE ELECTRON DENSITIES ON FUNCTIONAL GROUPS OF SOME HETEROCYCLIC MERCAPTAN DERIVATIVES

By

Á. RAUSCHER, HIGAZ NADER ALI, J. HORVÁTH, M. I. BÁN, I. BÁLINT

Institute of General and Physical Chemistry, Attila József University, Szeged, Hungary

(Received 25th April, 1981)

The inhibition effects of some heterocyclic mercapto derivatives on the corrosion behaviour of AISI 316 L stainless steel and pure iron in solutions containing chloride ion have been studied by means of a quasipotentiostatic polarization method. The determined corrosion parameters were compared with the electron densities on the sulfur atom of the functional group of the inhibitors, calculated by the CNDO/2 method. The electron density data and the measured corrosion parameters showed a correlation in tendency, proving the significance of the electron density on the donor atom in the inhibition process.

Introduction

The inhibiting action exerted by organic compounds on the dissolution of metals is attributed to adsorption interactions between the inhibitor molecule and the metal surface. Metal-inhibitor interactions may vary in type, but it is generally accepted that effective inhibition is linked with chemisorption involving charge transfer [1]. Most of the organic inhibitors have at least one polar functional group, the electron donor atom of which is responsible for the chemisorption process. In such a case the strength of the chemisorption bond is determined by the electron density on the donor atom and the polarizability of the functional group.

The importance of the electron density on the donor atom in the chemisorption during inhibition by various effective organic compounds has been discussed by HACKERMAN [2], DONAHUE [3, 4], RIGGS [5] and other authors.

Our aim was to study the correlation between the inhibition efficiency of some heterocyclic mercapto compounds and the calculated electron density data relating to the donor atoms.

Experimental

AISI 316 L stainless steel and high-purity iron* (Johnson—Matthey Ltd.) were used for the electrochemical investigations. The electrodes were employed in the form of cylinders. The stainless steel specimens were abraded with silicon-carbide paper to a 600-grit finish, degreased with acetone, rinsed in distilled water, then pickled in 15% HNO_3 and 5% HF solution at 353 K for 5 minutes, washed with a jet stream of tap water and rinsed in distilled water. The iron specimens were electropolished after mechanical polishing [6].

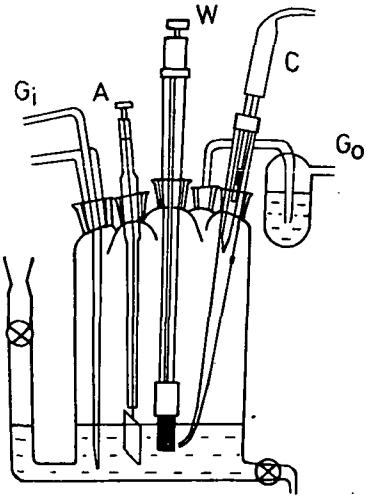

Fig. 1. Scheme of the electrochemical cell W Working electrode; C Saturated calomel electrode; A Auxiliary electrode; G_i Gas inlet; G_o Gas outlet

The inhibitors investigated were: 2-mercaptopyridine (2MP), 2-mercaptopyrimidine (2MPm), 2-mercaptobenzimidazole (2MBi), 2-mercaptobenzothiazole (2MBt), 2-mercaptobenzoxazole (2MBo) and 1-phenyl-5-mercaptotetrazole (1F5MT).

The inhibitor efficiency was determined at a constant concentration of $1 \cdot 10^{-3}$ mol dm^{-3} in a solution containing 0.1 mol dm^{-3} Cl^- ion. The chosen inhibitor was dissolved in methanol in such a concentration that 50 cm^3 of the prepared solution when diluted to 1 dm^3 gave the desired concentration of $1 \cdot 10^{-3}$ mol dm^{-3}. The uninhibited solution contained the same amount of methanol. The anodic behaviour of the AISI 316 L stainless steel was investigated at pH=1 and that of the iron at pH=7.

Deaeration was accomplished by bubbling highly-purified nitrogen gas through the solution. Nitrogen was also passed over the solution during the measurements.

The experiments were conducted in an electrolytic cell, shown in Figure 1. The potential of the specimen was measured against a saturated calomel electrode. The electrode potentials here are referred to the normal hydrogen electrode.

A PRT-100-1x Tacussel potentiostat was used for the polarization experiments. The specimens were polarized from the stationary potentials in the noble direction until (after the breakdown of the passive film) the current density reached a value of 50 μA cm^{-2}, and then in the active direction. The scanning rate was 0.3 V hr^{-1} (25 mV/5 min).

* The inclusions in ppm were stated by the manufacturers to be

Si	Mn	Cu	Mg	Al	Ag
5	3	2	2	1	1

Results

Electrochemical polarization data

The quasipotentiostatic polarization curves of AISI 316 L are shown in Figures 2 and 3. The most important electrochemical data derived from these Figures are listed in Table I.

From Figures 2 and 3 and from Table I it can be concluded that in highly acidic media (pH=1) all the investigated organic compounds inhibited both the active dissolution and the pitting corrosion of the stainless steel. In the inhibition of the active dissolution, 2MP proved to be the most effective. It significantly increased the anodic overvoltage and almost completely depressed the critical current density. Furthermore, in the presence of 2MP the corrosion potential was shifted in the

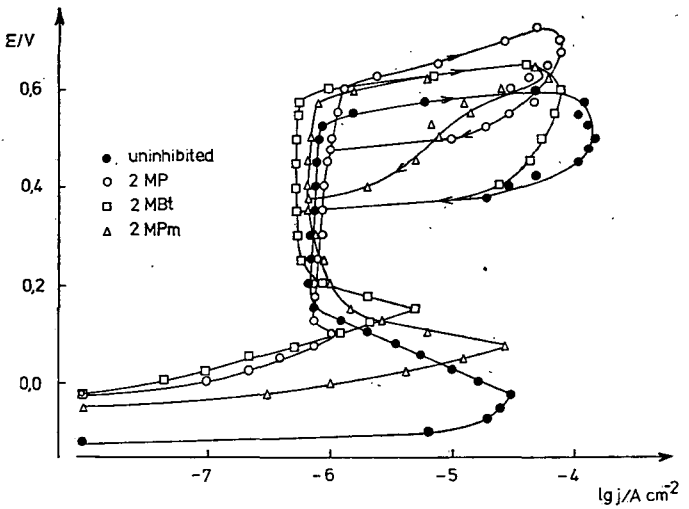

Fig. 2. Quasipotentiostatic anodic polarization curves of AISI 316 L stainless steel electrodes with 2MP, 2MBt and 2MPm; pH=1

Table I

Parameters characterizing the efficiency of inhibitors

Inhibitor	Corrosion potential E_{corr}/V	Passivation potential E_p/V	Critical current density j_{crit}/μA cm^{-2}	Breakdown potential E_b/V	Repassivation potential E_r/V
—	−0.125	0.15	30	0.525	0.35
2MP	−0.025	0.125	1.2	0.60	0.475
2MPm	−0.05	0.20	26	0.575	0.375
2MBi	−0.05	0.15	3.5	0.55	0.35
2MBt	−0.025	0.225	5	0.575	0.35
2MBo	−0.025	0.15	5	0.575	0.375
1F5MT	−0.05	0.15	4	0.60	0.35

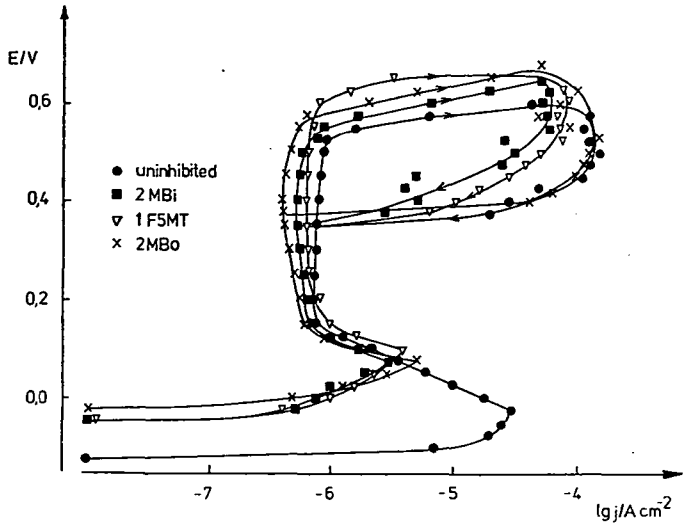

Fig. 3. Quasipotentiostatic anodic polarization curves of AISI 316 L stainless steel electrodes with 2MBi, 1F5MT and 2MBo; pH = 1

noble direction. 2MBi, 2MBt, 2MBo and 1F5MT showed a similar inhibition effect on the active dissolution, though they were less effective than 2MP. On the other hand, 2MPm displayed practically no inhibiting property.

The susceptibility of the stainless steel to pitting corrosion was most significantly depressed by 2MP. It shifted both the breakdown and the repassivation potentials in the noble direction. The rate of pit propagation was also the slowest in the presence of 2MP, since the arbitrary pitting current density of 50 μA cm^{-2} was reached at a potential more noble than the breakdown potential by 125 mV. The breakdown and repassivation potentials were likewise shifted in the positive direction by 2MPm and 2MBo, but these shifts were smaller than those resulting with 2MP. In the presence of the other organic inhibitors, 2MBi, 2MBt and 1F5MT, the breakdown potential was positively shifted in this sequence, while the repassivation potential was unchanged. With the exception of 2MP, the hysteresis ($E_b - E_r$) was slightly increased, that is the breakdown potential was changed more significantly than the repassivation potential.

Anodic quasipotentiostatic polarization curves obtained for pure iron in uninhibited and inhibited neutral solutions (pH = 7) are shown in Figure 4.

In the uninhibited solution passivation did not occur, whereas at a potential 150 mV above the corrosion potential the current density abruptly increased. 2MPm behaved similarly as in the case of the active dissolution of AISI 316 L. Rather than inhibiting, it accelerated the anodic dissolution of the iron. In the presence of the other compounds, different j_{crit} values were obtained. After the critical current was reached, the current density decreased in a very narrow potential region, and then at a higher electrode potential it increased again. 1F5MT and 2MP proved to be the most effective compounds for inhibition of the active anodic dissolution of iron: the lowest critical current densities were obtained at the least positive electrode potentials.

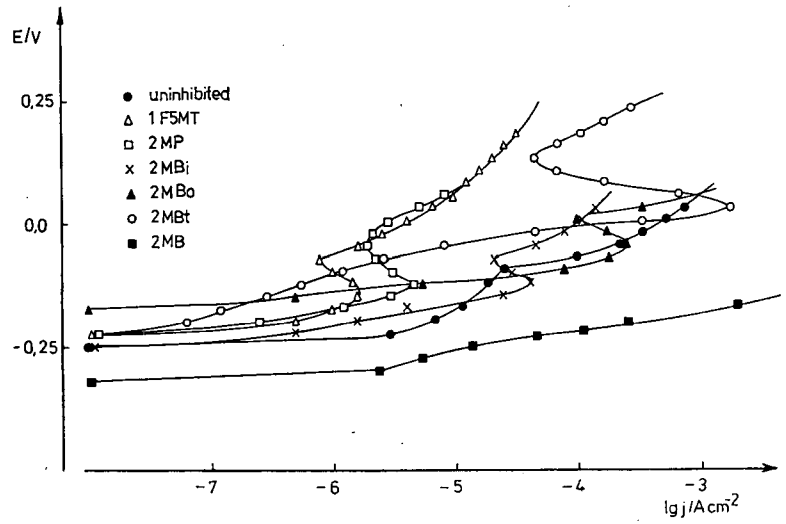

Fig. 4. Quasipotentiostatic anodic polarization curves of iron; pH=7

Electron density data

The electron densities on the sulfur atoms of the functional groups and on the ring hetero-atoms were calculated by the CNDO/2 method [7].

In the lack of exact geometrical data on the investigated heterocyclic mercaptans, data have been used that relate to similar molecules or to molecules with idealized structures constructed from known data on the corresponding molecular fragments and bonds [8].

The values of the net charges obtained from these calculations are presented in Table II.

Discussion

In Figure 5 the critical current densities and the breakdown potentials of stainless steel, determined in the presence of the investigated inhibitors at pH=1, are plotted *vs.* the values of the electron densities on the sulfur atoms (ϱ_S). It can be seen that the critical current density decreases with the increase of ϱ_S. However, the data on 1F5MT show a marked deviation from this correlation: the electron density on the sulfur atom is the largest in this compound, yet it does not exert the greatest influence on the critical current density.

There is no unambiguous correlation between the electron density data and the characteristic potentials of pitting (E_b and E_r). On the other hand, in the cases of 2MP and 1F5MT the values of ϱ_S are the highest, and correspondingly the most positive breakdown potentials are obtained.

The critical current densities determined for pure iron in the presence of the investigated compounds (which display marked inhibition effects) decrease with the

Table II

Inhibitor structures and electron density data

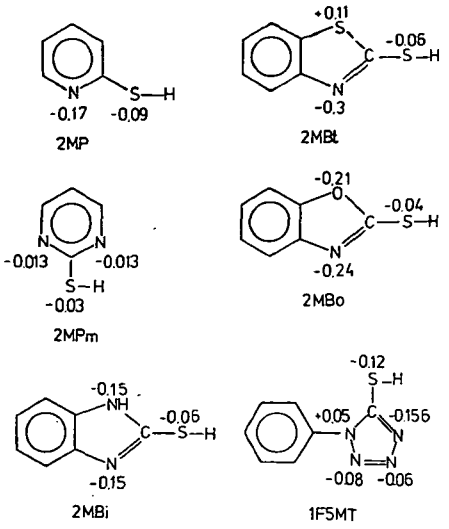

increase of ϱ_S, as in the case of stainless steel (Fig. 6). However, the potentials — at which the current densities once again sharply increase — do not shift in the positive direction with the increase of ϱ_S. These potentials can not be considered typical breakdown potentials, since they have more negative values the smaller the critical current densities at the least positive electrode potentials. It has been supposed that the decrease in the critical current density is due to the formation of a metal-inhibitor complex on the surface, while the sharp current increase is due to an intensive metal

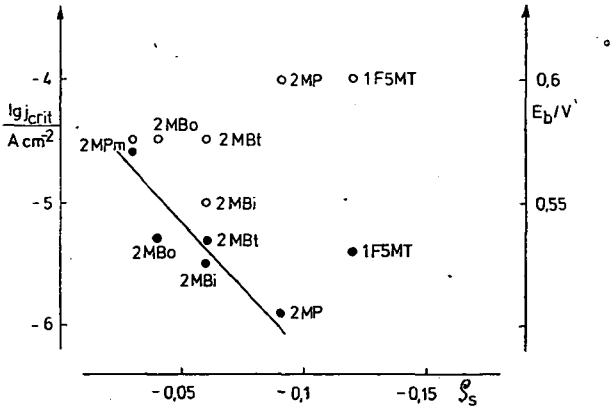

Fig. 5. Plot of the critical current densities (●) and the breakdown potentials (○) of stainless steel *vs.* electron densities on the sulfur atoms

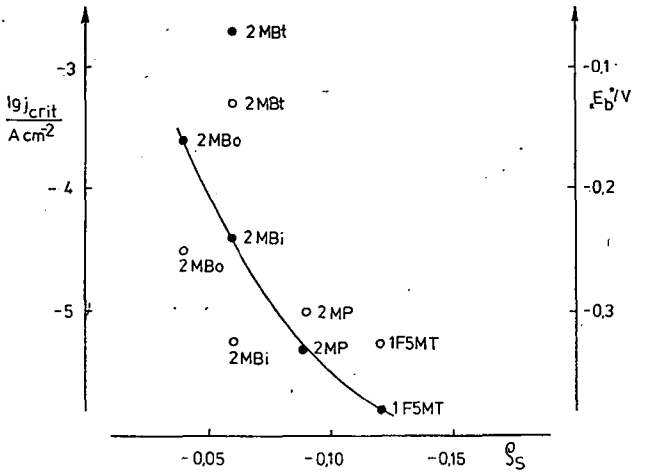

Fig. 6. j_{crit} (●) and E_b (○) *vs.* ϱ_S diagram for iron

dissolution owing to the desorption of the inhibitor. This assumption is supported by the surface concentration variation with the electrode potential of 1F5MT determined by laser Raman spectroscopy in conjunction with an electrochemical polarization method [9].

Conclusion

From the above discussion it is evident that completely unambiguous correlations have not been found between the experimental data characteristic of either the stainless steel or the iron and the electron densities of the investigated compounds. This fact can be attributed to several factors. First of all, it should be emphasized that the calculated ϱ_S values are only of a qualitative nature, showing tendencies or trends in the inhibition sequences, since there are several structural parameters which can be taken into consideration only approximately.

Furthermore, there are other factors (such as molecular area of the inhibitor projected onto the surface, the orientation of the molecules at the metal/electrolyte interface, the solubility of the metal-inhibitor complex or the composition and pH of the solution, the electrochemical conditions of metal surface, etc.) which play dominant roles in the inhibiting action. Nevertheless, correlations in tendency between the measured corrosion parameters and the calculated electron density data prove that the electronic charge on the sulfur atom does play an important role in the chemisorption during inhibition process, even if it cannot explain all the observed effects.

Acknowledgment

Thanks are due to Mr. Gy. Lendvay of the Central Research Institute for Chemistry for carrying out some preliminary calculations.

References

[1] *Fontana, M. G., R. W. Staehle:* Advances in Corrosion Science and Technology, Plenum Press, New York—London (1970), Vol. 1., p. 148
[2] *Ayers, Jr. R. C., N. Hackerman:* J. Electrochem. Soc., **110**, 507 (1963).
[3] *Donahue, F. M., K. Nobe:* J. Electrochem. Soc., **112**, 886 (1965); **114**, 1012 (1967).
[4] *Donahue, F. M., A. Akiyama, K. Nobe:* J. Electrochem. Soc., **114**, 1006 (1967).
[5] *Riggs, O. L., R. L. Every:* Corrosion, **18**, 262t (1962).
[6] *Sewell, P. B., C. D. Stockbridge, M. Cohen:* Can. J. Chem., **37**, 1813 (1959).
[7] *Pople, J. A., D. L. Beveridge:* Approximate Molecular Orbital Theory, McGraw-Hill, New York (1970).
[8] Tables of Interatomic Distances and Configurations in Molecules and Ions, The Chemical Society, Burlington House, London (1958).
[9] *Gál M., Rauscher Á., Higaz Nader Ali, Horváth J.:* Magy. Kém. Folyóirat (1981), in press.

ЗАВИСИМОСТЬ МЕЖДУ ОТНОСИТЕЛЬНЫМ ИНГИБИРУЮЩИМ ЭФФЕКТОМ КОРРОЗИИ И ЭЛЕКТРОННОЙ ПЛОТНОСТЬЮ ФУНКЦИОНАЛЬНЫХ ГРУПП НЕКОТОРЫХ ПРОИЗВОДНЫХ ГЕТЕРОЦИКЛИЧЕСКИХ МЕРКАПТАНОВ

А. Раушер, Хигаз Надер Али, Й. Хорват, М. Бан и И. Балинт

Квазипотенциостатическим поляризационным методом изучен ингибирующий эффект некоторых производных гетероциклических меркаптанов на коррозию нержавеющей стали AISI 316L и чистого железа в растворах содержащих ионы хлора. Найденные параметры коррозии сравнены с электронной плотностью на атоме серы функциональных групп ингибиторов, расчитанной методом CNDO/2.